HumanCoser: Layered 3D Human Generation via Semantic-Aware Diffusion Model

Yi Wang[1,†], Jian Ma[1,†], Ruizhi Shao[2], Qiao Feng[1], Yu-Kun Lai[3], Yebin Liu[2], Kun Li[1,*]
[1]Tianjin University, China [2]Tsinghua University, China
[3]Cardiff University, U.K

Figure 1. Our method can generate layered 3D humans guided by text prompts, which are physically-decoupled and structurally consistent. This allows our generated clothing to be reused, exchanging between digital avatars with different identities.

Abstract

The generation of 3D clothed humans has attracted increasing attention in recent years. However, existing work cannot generate layered high-quality 3D humans with consistent body structures. As a result, these methods are unable to arbitrarily and separately change and edit the body and clothing of the human. In this paper, we propose a text-driven layered 3D human generation framework based on a novel physically-decoupled semantic-aware diffusion model. To keep the generated clothing consistent with the target text, we propose a semantic-confidence strategy for clothing that can eliminate the non-clothing content generated by the model. To match the clothing with different body shapes, we propose a SMPL-driven implicit field deformation network that enables the free transfer and reuse of clothing. Besides, we introduce uniform shape priors based on the SMPL model for body and clothing, respectively, which generates more diverse 3D content without being constrained by specific templates. The experimental results demonstrate that the proposed method not only generates 3D humans with consistent body structures but also allows free editing in a layered manner. The source code will be made public. The project page is available for research purposes at http://cic.tju.edu.cn/faculty/likun/projects/HumanCoser.

† Equal contribution.
* Corresponding author.

1. Introduction

The generation of 3D humans with changeable clothing plays an important role in movies, games and AR/VR. Existing methods [10, 33, 37, 43, 44, 47] can only generate a single surface with coupled body and clothing, and thus cannot be edited and reused separately. In this paper, we aim to generate high-fidelity layered 3D humans with the ability to change clothes, as shown in Fig. 1.

Recently, owing to the high-quality image synthesis capability of pre-trained diffusion models [39], some methods [24, 33, 37] introduce a novel Score Distillation Sampling (SDS) strategy [39] to self-supervise the 3D human generation process. However, these methods ignore the diversity and self-occlusion of human shapes, which leads to inconsistencies in generated human structures. Furthermore, most data-driven 3D avatar generation methods [6, 11, 14, 18, 46, 53] generate 3D clothed humans in a coupled manner, and as a result, clothing cannot be exchanged between arbitrary bodies. Overall, the aforementioned methods fail to ensure structural consistency and lack the capability to generate and edit bodies and clothes in a layered and flexible manner.

This paper introduces HumanCoser, a novel framework based on a physically decoupled semantic-aware diffusion model. It aim to generate high-quality physically-decoupled 3D clothed humans with consistent body structure in a layered manner, guided by text. To achieve accurate geometric alignment between decoupled body and clothing, we present a 3D implicit deformation field using SMPL [23] vertex prediction, leveraging SMPL-X [31] as a body proxy for matching with clothing. Additionally, we incorporate a layered shape prior to ensure structural consistency in the generation of 3D human bodies and clothes. To enhance details, we introduce a normal prediction network for smooth normals, combined with optimized spherical harmonic lighting. To ensure semantic consistency with the text, we propose a clothing semantic confidence strategy for 3D implicit fields, employing an implicit 3D semantic-confidence prediction network. This strategy removes redundant non-clothing content and enhances robustness through the addition of Gaussian noise. Hence, the proposed HumanCoser ensures structural consistency while allowing for variability in body clothing.

Our main contributions are summarized as follows:

- We propose a layered 3D human generation framework with a semantic-aware diffusion model. To our best knowledge, this is the first work that is truly physically-decoupled and supports the generation of structurally consistent human bodies and clothing. We also introduce a decoupled shape prior to generate structurally consistent 3D content.
- We propose a semantic-confidence strategy for 3D implicit fields to improve the semantic consistency of clothing generation. The strategy not only improves the semantic consistency of the clothing but is also generalizable to the enhancement of 3D semantics for other wearable outfits of humans.
- We propose a 3D implicit deformation method based on SMPL vertex prediction to achieve the geometric matching of human bodies and clothing in an implicit manner, so that the clothing can be transferred between different human subjects.
- We propose normal consistency constraints and optimized spherical harmonic lighting to improve the details of both geometry and appearance.

2. Related Work

Text-guided 3D Content Generation. CLIP-Forge [42] and Dream-Field [15] optimize Neural Radiance Fields (NeRFs) to generate 3D shapes by aligning the embedding of the generated image with the text embedding in the space of the image-text model CLIP. CLIP-mesh [27] also uses CLIP to optimize meshes to represent 3D shapes. However, by directly generating images aligned with text in CLIP space, it is not possible to generate highly realistic images. Recently, diffusion modeling [29, 39, 40] has seen rapid growth due to its excellent performance in synthesizing high-quality images. DreamFusion [34] proposes Score Distillation Sampling (SDS) based on a pre-trained diffusion model [39] to optimize trainable NeRFs. Magic3D [22] uses a 2-stage training strategy to bootstrap 3D texture networks to optimize 3D content generation. Although the above diffusion-based 3D generation models have some 3D generation capability, the generation of 3D human is a challenge for the above methods due to the complexity of their shapes and the diversity of their poses.

Text-guided 3D Human Generation. AvatarCLIP [12] initializes the 3D human body shape via a VAE (Variational Autoencoder) encoder, and then performs geometric shaping and texture generation guided by an image-text model [35]. However, since the method focuses on shaping localized structures, it lacks in the generation of global structures such as skirts, long hair and loose clothing. In addition, Latent-NeRF [24] and TADA [21] both utilize pre-trained text-to-image diffusion models for 3D avatar generation work. In particular, Latent-NeRF [24] employs a Sketch-Shape to constrain the generation of the diffusion model, but the results of this method lack details due to the lack of optimization of normals and illumination. TADA [21] is limited by the representation ability of the confined mesh, and thus cannot represent non-convex structures or transparent materials well. Neither of the above methods can generate 3D avatars with layered bodies and clothing. In addition, although the HumanLiff [13] method can generate a layer-wise 3D human body based on the diffusion model in a layer-by-layer manner, the features of

Method	Multilayer	Geometry (non-skin tight)	Clothing Transfer	Reusability
AvatarCLIP [12]	✗	✗	✗	✗
TADA [21]	✗	✗	✗	✗
Latent-NeRF [24]	✗	✓	✗	✗
HumanLiff [13]	✓	✓	✗	✗
Ours	✓	✓	✓	✓

Table 1. Comparison of 3D human generation methods, including layered generation, geometric complexity, clothing transfer and clothing reusability.

each layer depend on the tri-plane features of the previous layer, which makes the features of each layer coupled and not conducive to the editing and reuse of each layer separately. In contrast, our method can generate realistic bodies and clothing by predicting normals and improved spherical harmonic lighting. Moreover, we can generate text-consistent clothing by optimizing the semantic-confidence of the clothing and generate layered avatars for complex poses driven by an implicit deformation network based on SMPL. We summarize the main differences between our work and related work in Tab. 1.

3. Overview

Our goal is to generate realistic 3D humans with consistent body structure guided by text in a layered manner. The overall framework of our approach is shown in Fig. 2. Our approach contains two stages: (1) decoupled generation stage of body and clothing (Sec. 4.2), and (2) matching and synthesis stage of body and clothing (Sec. 4.3).

Decoupled Generation Stage. We introduce the layered shape prior to the human body and clothing combined with the predicted normals and their regularization constraints to generate the human body and clothing in a layered manner.

Matching and Synthesis Stage. In order to accurately match and synthesize the layer-generated human body and clothing, firstly, we propose a semantic confidence strategy for 3D implicit fields and design a 3D semantic weight prediction network (Sec. 4.3.1) to fine-tune the geometry of the pre-trained clothing layers to be consistent with the text prompts. Secondly, we utilize a SMPL-driven implicit field deformation network (SID Net) to fine-tune the body geometry to fit the clothing (Sec. 4.3.2).

4. Method

4.1. Preliminaries

Our approach incorporates three key components in the generation process, each defined as follows:

3D Implicit Representation. Neural Radiance Field (NeRF) [26] represents the 3D scene via an implicit function and it uses a multilayer perceptron (MLP) that maps each spatial point $\mathbf{x} \in \mathbb{R}^3$ to density and an RGB color (δ, c):

$$F_\theta(\gamma(\mathbf{x})) = (\sigma, c), \tag{1}$$

where $\gamma(.)$ is the frequency encoder. We render the scene using the volume rendering equation [26]. First, rays projected from the center of the camera through the image pixels are generated, and then the predicted color $C(\mathbf{r})$ along each ray $\mathbf{r}$ is computed:

$$\begin{aligned} C(\mathbf{r}) &= \sum_i w_i \mathbf{c}_i, \\ w_i &= \alpha_i \prod_{j<i} (1-\alpha_j), \end{aligned} \tag{2}$$

where $\alpha_i = 1 - \exp\left(-\sigma_i \left\|\mathbf{x}_i - \mathbf{x}_{i+1}\right\|\right)$ and $\left\|\mathbf{x}_i - \mathbf{x}_{i+1}\right\|$ is the interval between sample i and $i+1$. w_i is the weight of the ith sampling point [26]. c_i and σ_i is the predicted color and density of the ith sampling point [26].

Score Distillation Sampling (SDS)**.** SDS is based on the text-guided diffusion model ϕ [39, 41]. We employ the pre-trained Stable Diffusion [39] for optimizing the NeRF field representation of 3D human. For the NeRF model parameterized by θ, SDS computes the gradient of the parameter θ for the NeRF by:

$$\nabla_\theta \mathcal{L}_{SDS}(\phi, x) = \mathbb{E}_{t,\epsilon}\left[w(t)\left(\epsilon_\phi\left(x_t; y, t\right) - \epsilon\right)\frac{\partial x}{\partial \theta}\right], \tag{3}$$

where x is the result of the NeRF differentiable renderer rendering, $w(t)$ is a weighting function that depends on the noise level t, x_t denotes a noisy image with noise level t, and y is the text embedding.

Human Representation. We utilize the expressive SMPL-X [30] as a shape prior, which captures not only shape and pose variations of the entire body, but also knuckles and facial expressions. Given the parameters of the identity body shape $\boldsymbol{\beta} \in \mathbb{R}^{|\boldsymbol{\beta}|}$, $\boldsymbol{\theta} \in \mathbb{R}^{3n_k+3}$ and facial expression $\boldsymbol{\psi} \in \mathbb{R}^{|\psi|}$, SMPL-X is defined as a differentiable mesh. In order to drive body for matching clothing by using SMPL-X, we add an additional set of vertex offsets $\boldsymbol{O} \in \mathbb{R}^{n_v \times 3}$ for vertex editing, and define the model as:

$$M(\boldsymbol{\beta}, \boldsymbol{\theta}, \boldsymbol{\psi}, \boldsymbol{O}) = \mathrm{LBS}\left(T_P(\boldsymbol{\beta}, \boldsymbol{\theta}, \boldsymbol{\psi}, \boldsymbol{O}), \mathbf{J}(\boldsymbol{\beta}), \boldsymbol{\theta}, \mathcal{W}\right), \tag{4}$$

where $\mathrm{LBS}(.)$ is the standard linear skinning function [28], $T_P(.)$ is the stationary pose mesh, $\mathbf{J}(\boldsymbol{\beta}) \in \mathbb{R}^{3K}$ is the corresponding keypoint location, and $\mathcal{W} \in \mathbb{R}^{N \times K}$ is a set of mixing weights.

4.2. Decoupled Generation of Bodies and Clothing

Fig. 2(a) shows our framework for decoupled generation of bodies and clothing. To enable easy editing and transfer of the clothing for 3D avatars, we extract knowledge from the pre-trained diffusion model to shape the body and clothing in layers based on the NeRF representations.

Layered Geometric Prior. In order to accelerate the convergence of NeRF and provide reasonable initial inputs

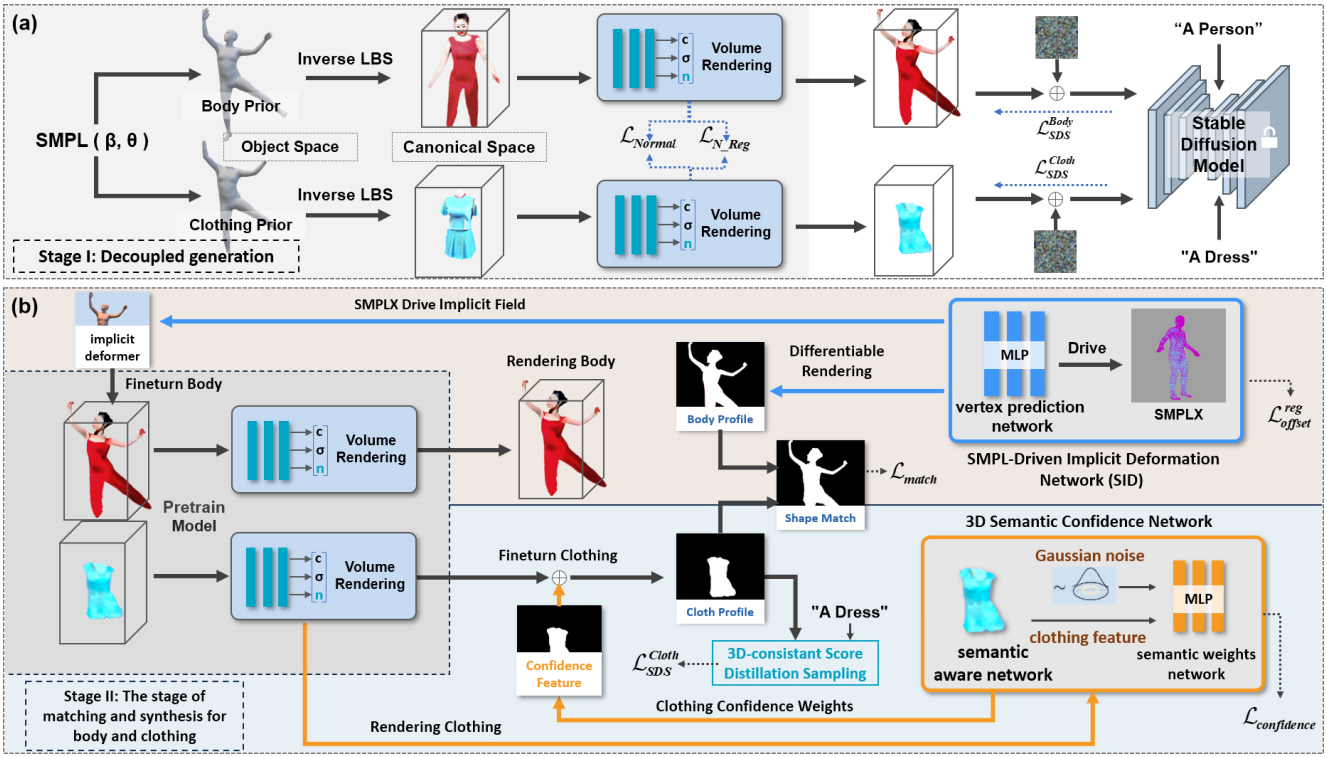

Figure 2. Illustration of our framework for generating the clothes and body of an avatar in a layered manner. (a) shows the decoupled generation of the initial body and clothing, and (b) shows the matching and synthesis of the generated body and clothing.

for the diffusion model, we use parametric human model SMPL [23] as the geometric prior $\mathcal{M}_{body}^{prior}$ to initialize the density of the body. Also based on the observation that clothing is usually fitted to the inner body of a person, we exclude the head, hands and feet from the standard SMPL model as the geometric prior $\mathcal{M}_{cloth}^{prior}$ for clothing.

Canonical Spatial Sampling and Density Initialization. In order to minimize the inconsistency of body structure due to self-occlusion of body, and at the same time better provide standardized input for the optimization of texture and geometry of Diffusion. Firstly, for each NeRF sampled point p, we obtain p's nearest neighbor point set v_c based on the mesh $M(\boldsymbol{\beta}, \boldsymbol{\theta}, \boldsymbol{\psi}, \boldsymbol{O})$ (Eq. (4)), We then use the transformation matrix T_{skel} of v_c to project p to the canonical space to obtain p' for the subsequent feature query and volume rendering in the canonical space. Secondly, we initialize the density of the neural radiance field using the layered geometric prior $\mathcal{M}_{body}^{prior}$, $\mathcal{M}_{cloth}^{prior}$ respectively.

Specifically for the point p' that transforms from observation space to canonical space, we compute the signed distance $d(.)$ between p' and p''s nearest neighbor on the surface of $\mathcal{M}_{body}^{prior}$ and $\mathcal{M}_{cloth}^{prior}$. The signed distance field $d\left(p', \mathcal{M}^* \subset \left\{\mathcal{M}_{body}^{prior}, \mathcal{M}_{cloth}^{prior}\right\}\right)$ is used to initialize the density field:

$$
\begin{aligned}
v_x &= \frac{1}{\mu} \operatorname{sigmoid}\left(-\frac{d\left(x, \mathcal{M}^*\right)}{\mu}\right), \\
\delta_x &= \max\left(0,\ \operatorname{softplus}^{-1}\left(v_x\right)\right),
\end{aligned}
\tag{5}
$$

where μ is a hyperparameter controlling the sharpness of the geometric boundary with a default value of 0.05.

Predicting Smooth Normals. Since the geometric surface normals $\mathbf{n}$ generated by NeRF through the gradient of the density field are very noisy, it can lead to poor coloring of the clothing surface. In order to make the generated surface normals smoother and at the same time shape the avatar more accurately, we compute the predicted normal loss between the surface normals $\mathbf{n}'$ predicted by the MLP and $\mathbf{n}$:

$$
\mathcal{L}_n = \sum_i w_i \left\|\mathbf{n}_i' - \mathbf{n}_i\right\|, \tag{6}
$$

where w_i is the weight of the ith sampling point, which follow the definition of Eq. (2). The predicted surface normals enable a finer construction of geometric and textural details consistent with the target text.

Meanwhile, in order to regularize the normal and to reduce redundant semantically generated artifacts, a loss of regular constraints on the predicted normals is added:

$$
\mathcal{L}_n^{reg} = \sum_i w_i \left(1 - \sum \mathbf{n}_i' \cdot \mathbf{n}_i\right), \tag{7}
$$

where the weights w_i is the weight of the ith sampling point. Combining the predicted normal loss, normal regularization loss and SDS loss, the overall loss for body and clothing is formulated in a layered manner in the first stage as:

$$\mathcal{L}_{\text{stageI}} = \lambda_{\text{SDS}}^{body}\mathcal{L}_{\text{SDS}}^{body} + \lambda_{\text{SDS}}^{cloth}\mathcal{L}_{\text{SDS}}^{cloth} + \lambda_n\mathcal{L}_n + \lambda_n^{reg}\mathcal{L}_n^{reg}, \tag{8}$$

where $\mathcal{L}_{\text{SDS}}^{body}$ and $\mathcal{L}_{\text{SDS}}^{cloth}$ are defined on the canonical space:

$$\begin{aligned}\mathcal{L}_{\text{SDS}}^{body} &= \mathbb{E}_{t,\epsilon}\left[w(t)\left(\epsilon_\theta\left(x_t^{body}, y, t\right) - \epsilon\right)\frac{\partial x}{\partial \theta}\right], \\ \mathcal{L}_{\text{SDS}}^{cloth} &= \mathbb{E}_{t,\epsilon}\left[w(t)\left(\epsilon_\theta\left(x_t^{cloth}, y, t\right) - \epsilon\right)\frac{\partial x}{\partial \theta}\right].\end{aligned} \tag{9}$$

4.3. Matching and Synthesis of Body and Clothing

Fig. 2(b) shows our framework for body and clothing matching and synthesis. In the process of optimal matching of body and clothing, we first introduce a confidence network of 3D implicit fields for predicting semantic confidence features of clothing in NeRF fields. The confidence features are fused with the color features rendered by NeRF and input into the pre-trained diffusion model to compute the self-supervised SDS loss to further optimize the appearance of the clothing. Then, the shape matching loss between the pre-trained clothing and body is computed, and the gradient of the matching loss is utilized to update the SMPL-based implicit deformation network, which drives the body to deform finely for shape-matching with the clothing.

4.3.1 3D Semantic Confidence Network

In order to accurately obtain the shape of clothing, we introduce a 3D confidence network to eliminate the parts that are inconsistent with the semantics of clothing.

As shown in the 3D confidence network framework in Fig. 2(b), the confidence network consists of a semantic-aware network and a 3D semantic weight prediction network. Firstly, the pre-trained semantic-aware network $F_{sa}(.)$ consists of a cascaded text-guided semantic segmentation network. It perceives and obtains the features of the clothing $\{f_s \mid f_s \in \mathcal{F}_{cloth} \wedge f_s \notin \mathcal{F}_{other}\}$ generated in the first stage according to the clothing prompts, where $\mathcal{F}_{cloth}$ and $\mathcal{F}_{other}$ are the clothing feature portion and the non-clothing feature portion, respectively, of the single-frame rendered image of the clothing. Then, based on the perceived clothing features f_s, the clothing semantic confidence s_c of each ray is predicted by the 3D semantic weight network $F_{sw}(.)$ composed by MLP, as follows:

3D Semantic Prediction for Clothing. We predict the clothing semantic value τ_i^s regressed by the sampling point p_i on the ray:

$$\tau_i^s = F_{sw}\left(\mathbf{\Phi}, p_i, \mathbf{N}\right), \tag{10}$$

where $\mathbf{\Phi}$ denotes the parameters of the learnable semantic weight network and $\mathbf{N}$ is the Gaussian noise of the input semantic weight network to improve the robustness of the semantic prediction.

Confidence Prediction for Clothing. For each ray, the clothing semantic confidence s_c can be obtained by approximate integration:

$$\begin{aligned}s_c &= \sum_i \mathrm{O}_i, \mathrm{O}_i = \sigma_i \prod_{j<i}\left(1-\sigma_j\right), \\ \sigma_i &= 1 - \exp\left(-\tau_i^s \left\|p_{i+1} - p_i\right\|\right),\end{aligned} \tag{11}$$

where $p_{i,}$, p_{i+1} are two adjacent sampling points spaced on a ray. Finally, the loss of confidence $\mathcal{L}_{\text{confidence}}$ is calculated:

$$\mathcal{L}_{confidence} = \mathcal{L}_{huber}\left(s_c - f_s\right), \tag{12}$$

where s_c is the clothing semantic confidence predicted by the semantic weight network $F_{sw}(.)$, f_s is the clothing feature perceived by the pre-trained semantic awareness network $F_{sa}(.)$, and a smoothed loss function $\mathcal{L}_{huber}(.)$ [7] is used to obtain robustness to outliers.

The 3D semantic weight network $F_{sw}(.)$ can more accurately optimize the 3D semantics of the clothing in the NeRF field by perceiving the semantic features f_s of the clothing in multiple views.

4.3.2 SMPL-driven Implicit Field Deformation Network

In order to perform fine deformation of the body shape to fit the clothing, we introduce the SMPL-driven implicit deformation network (SID Net), as shown in Fig. 2(b). Furthermore, for precise body editing, we use SMPL-X [31] for our body shape prior and add learnable vertex offsets o for each shape prior. At the same time, we use the vertex prediction model $o = F_v(v)$ to predict the offset o of each vertex v of the SMPL shape prior. The specific implementation of SMPL to drive the body to match the clothing is as follows:

Optimizing vertices. Given the body SMPL parameters $(\boldsymbol{\beta}, \boldsymbol{\theta})$, the vertex offset $F_v : v \rightarrow o$ and the camera parameter ρ, we render a priori mesh of the body as a binary mask image $\mathcal{R}_m\left(M_{body}(\boldsymbol{\beta}, \boldsymbol{\theta}, o), \rho\right) \rightarrow I_{smpl}^{body}$, where $\mathcal{R}_m$ is a differentiable raster renderer. At the same time, we render a priori meshes of the clothing as binary mask images (where we use the SMPL model excluding vertices of the head, hands and feet) $\mathcal{R}_m\left(M_{cloth}(\boldsymbol{\beta}, \boldsymbol{\theta}), \rho\right) \rightarrow I_{smpl}^{cloth}$. Then, since the body mesh should be within the region where the clothing masks I_{mask}^{cloth} rendered by NeRF and I_{smpl}^{cloth} are merged, we perform the optimization using the following loss:

$$\mathcal{L}_{match} = \mathcal{L}_{huber}\left(I_{mask}^{cloth} + I_{smpl}^{cloth} - I_{smpl}^{body}\right), \tag{13}$$

where $\mathcal{L}_{huber}(.)$ [7] is a smoothed loss function. Also to smooth the predicted vertex offsets, we introduce a regularization loss for the vertex offset o:

$$\mathcal{L}_{offset}^{reg} = \|o\|_2, \tag{14}$$

where o contains the predicted vertex offsets for all vertices. Then, we update the vertex prediction model $F_v : v \rightarrow o_{opt}$ using the gradient of the $\mathcal{L}_{match}$ loss to obtain the optimized vertex offsets o_{opt} for optimizing the implicit geometry of the body.

Shape Matching. We are inspired by the method [54] to generalize the LBS (Linear Blend Skinning) deformation of the vertices of SMPL to the entire NeRF implicit space. Specifically, given a SMPL mesh $M(\theta, \beta, o) \rightarrow$ v with shape and pose parameters θ, β and vertex offsets o, a point p in the canonical space of the NeRF can be transformed by using the following method:

$$\sum_{\mathrm{v}_i \in \mathcal{N}(\mathrm{p})} \frac{\omega_i(\mathrm{p})}{\omega(\mathrm{p})} \mathrm{M}_i\left(0, \theta^c, 0, o\right) \mathrm{p} \rightarrow \mathrm{p}^{offset}, \tag{15}$$

where $\mathrm{M}_i(.) \in \mathbb{R}^{4\times4}$ is the transformation matrix in canonical space, and θ^c is the transformation from pose θ in observation space to the pose in canonical space. $\mathcal{N}(\mathrm{p})$ is the set of nearest-neighbor vertices of p in v. Furthermore, the weights of the transformations are:

$$\begin{aligned} \omega_i(\mathrm{p}) &= \exp\left(-\frac{\left\|\kappa_{nn(\mathrm{p})} - \kappa_i\right\|_2 \|\mathrm{p} - \mathrm{v}_i\|_2}{2\sigma^2}\right), \\ \omega(\mathrm{p}) &= \sum_{\mathrm{v}_i \in \mathcal{N}(\mathrm{p})} \omega_i(\mathrm{p}), \end{aligned} \tag{16}$$

where $\mathcal{N}(\mathrm{p})$ contains the indexes of p's nearest neighbor vertices in v, and κ_i is the mixing weight of v_i and is constant. With the above transformations, we finally transform the NeRF space point p of the body to p^{offset} in order to fine-tune the body contour to match the clothing, and the synthesized effect is shown in Fig. 2(b).

The overall loss for matching and synthesizing the body and clothing in the second stage is as follows:

$$\begin{aligned} \mathcal{L}_{\text{stageII}} = \lambda_{confidence}\mathcal{L}_{confidence} \\ + \lambda_{match}\mathcal{L}_{match} + \lambda_{reg}\mathcal{L}^{reg}_{offset}. \end{aligned} \tag{17}$$

5. Experiments

In this section, we assess the efficacy of our proposed layered avatar generation framework. We commence by providing implementation details in Sec. 5.1, followed by a succinct overview of the compared methods in Sec. 5.2. Subsequently, quantitative comparisons, inclusive of a user study, are presented in Sec. 5.3. Qualitative results, illustrating comparisons between state-of-the-art (SoTA) methods and our approach, are discussed in Sec. 5.4. Finally, an ablation study is presented in Sec. 5.5.

5.1. Implementation Details

Our framework is implemented based on Stable Diffusion [39] and NeRF [26] components, and it is trained and evaluated on a single NVIDIA 3090. For the decoupled generation stage of layered avatars: 10,000 and 15,000 iterations are needed for the 3D appearance of the body and clothing. In terms of the matching and synthesis stage of the layered avatar, the decoupled clothing is fine-tuned using a confidence network for 3,000 iterations, followed by 5,000 iterations of shape-matching training.

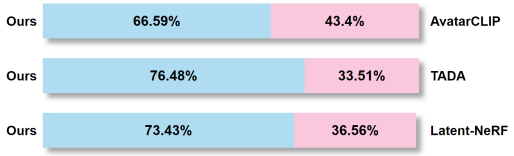

Figure 3. Quantitative results. Our method and methods [12, 21, 24] are evaluated by using the method [17] to measure the visual quality of the generated 3D content, where higher scores are better.

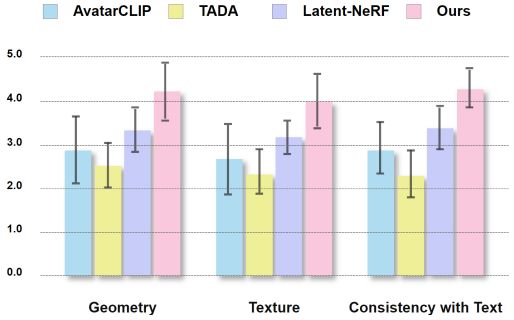

Figure 4. User study. We investigated user evaluations on geometric and texture quality, as well as consistency with text prompts.

5.2. Comparison Methods

We compare our approach with four SoTA methods. (1) AvatarCLIP [12] uses pre-trained vision-language CLIP model to guide NeuS [45] for 3D avatar generation; (2) TADA [21] creates 3D avatars from text by using hierarchical rendering with score distillation sampling; (3) Latent-NeRF [24] introduces sketch shape loss based on 3D shape guidance to supervise the training; (4) HumanLiff [13] firstly generates minimally clothed humans, represented by tri-plane features, in a canonical space and then progressively generates clothes in a layer-wise manner. HumanLiff is the most similar work to our method, aiming to generate layered human-body avatars.

5.3. Quantitative Results

This section quantitatively compares the proposed method with [12, 21, 24]. Inspired by the method [17], we render humans as images and then evaluate them using text-to-image metrics as no quantitative metrics directly evaluate the quality of text-to-3D generation. Fig. 3 demonstrates the superior performance of our method compared to [12, 21, 24] in generation quality, even when employing a coupled generation approach.

In addition, we perform a user study comparing our avatar generation with those of SoTA methods [12, 21, 24],

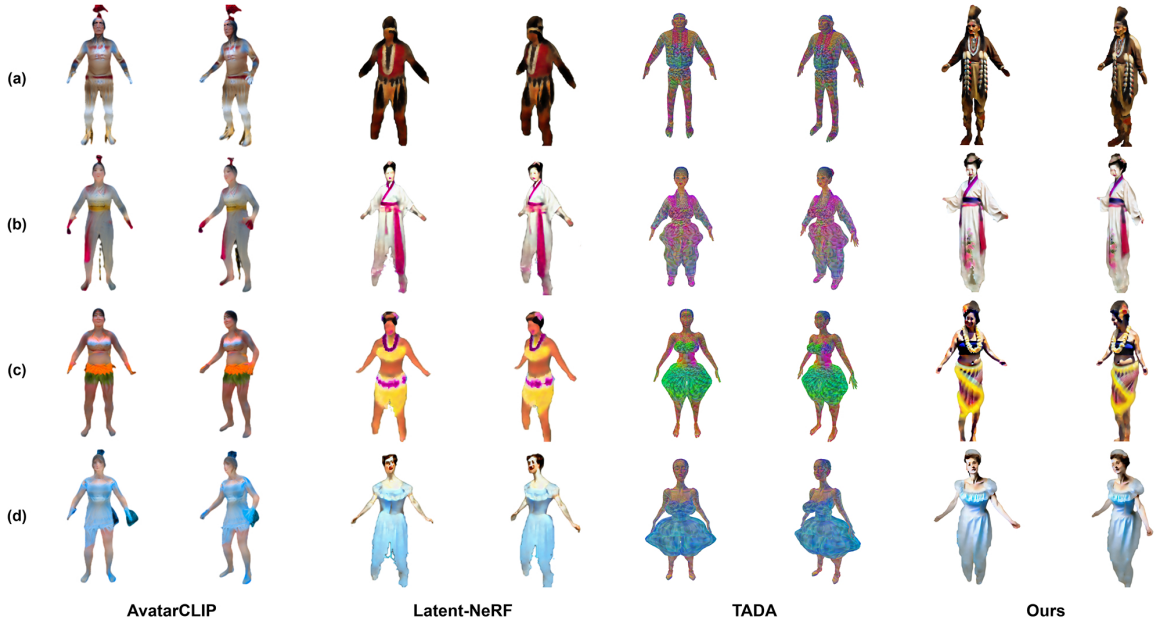

Figure 5. Qualitative comparison with coupled generation methods [10, 12, 21]. (a) prompt: "A north American Indian chief in full regalia", (b) prompt: "A Chinese lady wearing a gauzy hanfu", (c) prompt: "A Hawaiian woman wearing a hula skirt", (d) prompt: "A French woman wearing a light blue crinoline dress".

as shown in Fig. 4. Our approach achieves best scores across all three metrics, suggesting superior generative quality in both geometry and texture.

5.4. Qualitative Results

Fig. 5 qualitatively compares ours with text-guided 3D generation methods [12, 21, 24]. Considering that the methods [12, 21, 24] are based on coupled generation, we provide a coupled generation model for comparison. We render the model as multiple views for comparison. As shown in Fig. 5, although AvatarCLIP [12] generates view-consistent human bodies, it demonstrates limitations in effectively modeling global structures, such as skirts and long hair. Latent-NeRF [24] exhibits a limitation in its capacity to finely generate both geometry and texture. TADA [21]'s accuracy depends on the density of the mesh, and the discrete representation affects its geometric appearance. So, methods [12, 21, 24] exhibit deficiencies, either in the representation of geometric details or in the portrayal of fine textures. In contrast, our method produces humans characterized by enhanced geometric details, including loose clothing and diverse long hair, along with finer textures.

In addition, Fig. 6 illustrates the comparison of the layered 3D human generation approaches. HumanLiff [13] stands out as the most akin work to our method, employing a layer-by-layer generation approach. However, it lacks the capability to change clothes, as illustrated in the top row. HumanLiff generates a clothed human body by relying on a minimally-clothed human body. Instead, our approach demonstrates the ability to generate the body and clothing independently, as depicted in the second row. Subsequently, it engages in the matching of clothing and body, showcased in the third row. Finally, our method excels in the process of changing and reusing clothing, as illustrated in the last row.

Our method supports the transfer and matching of clothing between bodies in different shapes.

Clothing Transfer. Fig. 7 evaluates the effectiveness of our model in clothing transfer by exchanging avatars' clothes (left/right). In this case, the layered avatars are generated based on different SMPL shapes θ with the same pose β. We transfer the clothing layer of avatar left to the body layer of avatar right and vice versa: $\left(\text{cloth}^{\text{avatar left}} \rightarrow \text{body}^{\text{avatar right}}, \text{cloth}^{\text{avatar right}} \rightarrow \text{body}^{\text{avatar left}}\right)$, respectively. Fig. 7 illustrates that our model excels in adaptly shaping a match between the body and clothing layers, facilitating the transfer of the same clothing layer across different identity-based body layers.

Pose-Driven Generation. Fig. 8 demonstrates the effectiveness of pose-driven layered humans by applying various poses and identities to both the body and clothing layers. The incorporation of layered shape priors and implicitly deformed modules is noted for its contribution to improving the convergence of both body and clothing layers, ensuring appearance consistency with the given text prompt. Fur-

HumanLiff currently does not provide the official implementation, and hence we compare with the visual results presented in [13]

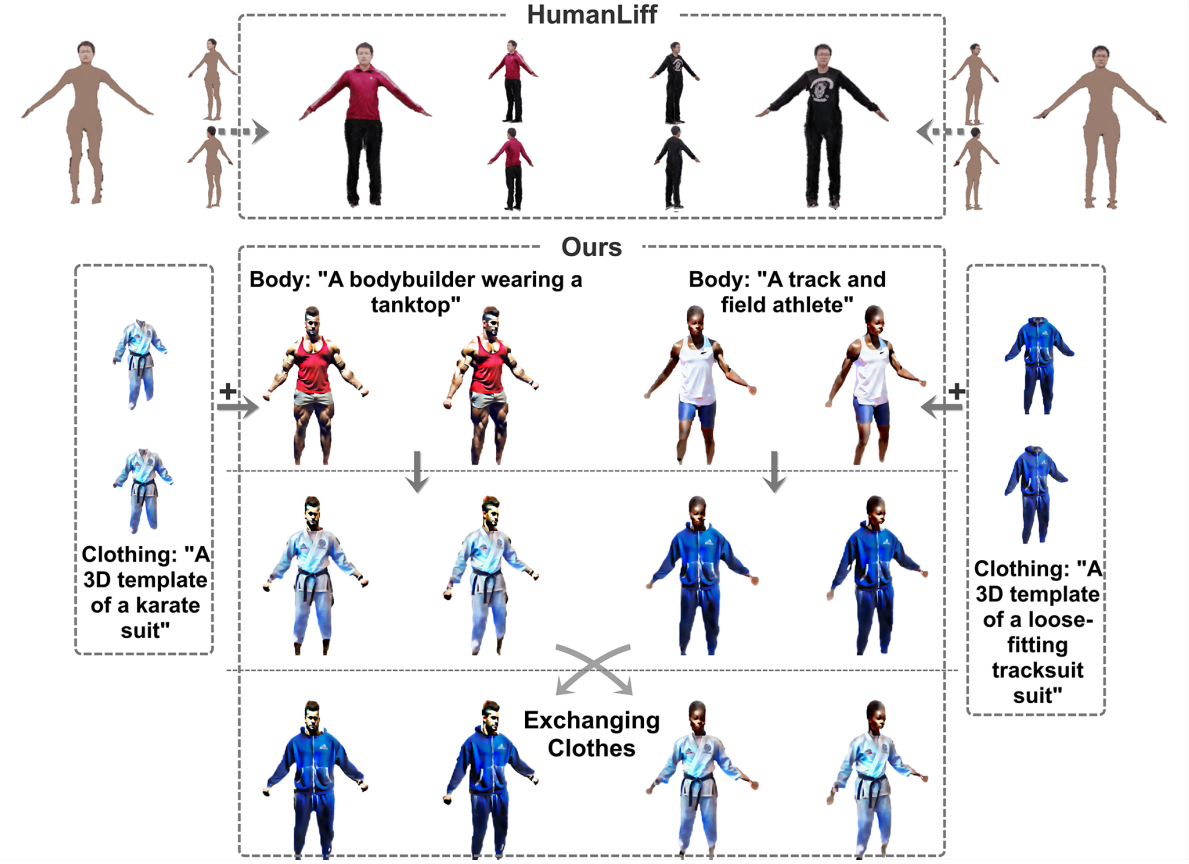

Figure 6. Qualitative comparison with a layered method [13].

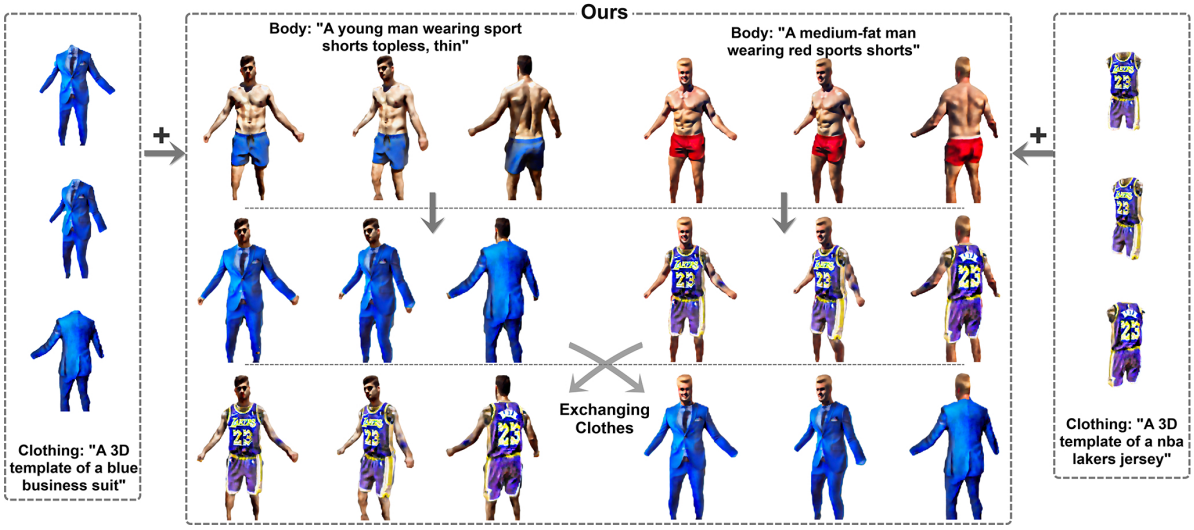

Figure 7. The effectiveness of clothing transfers.

thermore, these elements facilitate synchronized transformations in the structural aspects of both body and clothing layers, particularly when responding to intricate poses.

5.5. Ablation Study

Effect of Layered Shape Prior. To verify the effectiveness of the layered shape prior, we generate humans with or without the shape prior. Figs. 9 (a, b) show that when

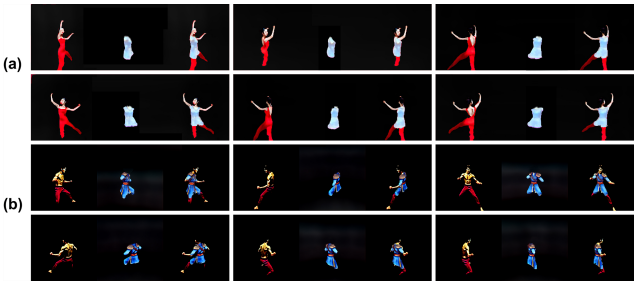

Figure 8. The effectiveness of Pose-Driven Generation.

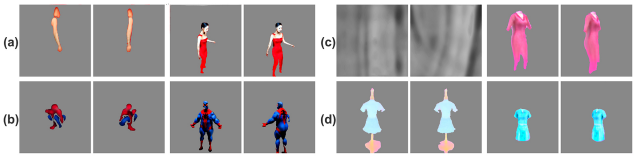

Figure 9. Ablation study on the effectiveness of layered shape constraints. (a),(b) are evaluations of the effectiveness of the layered shape prior for body generation. (c),(d) are evaluations of the effectiveness of the layered shape prior for clothing generation.

Figure 10. Ablation study on the effectiveness of semantic-confidence modules.

we remove the layered shape prior, the model seems not to converge correctly to a reasonable human body shape and pose. This is due to the complexity of the human body structure and self-occlusion. Additionally, the elimination of the layered shape prior during the clothing generation process leads to either an inability to converge to a well-defined geometry, as depicted in Fig. 9 (c), or suboptimal convergence in both geometry and texture, exemplified in Fig. 9 (d). Hence, the layered shape prior ensures that the model converges to the correct shape.

Effect of Semantic-Confidence Modules. To validate the effectiveness of the semantic-confidence module, we employ the direct text-guided generated dresser model as the initial state and iteratively optimize it using the confidence module. Fig. 10 shows that the confidence module can eliminate the non-clothing semantic generated content, and thus maintain consistency with clothing text prompts.

6. Conclusion and Limitations

Conclusion. In this paper, we propose a layered 3D human generation framework based on a semantic-aware diffusion model to generate bodies and clothing, and the clothing can be changed and reused between different individual bodies. The key idea revolves around the implementation of a physically dual generative branching system, wherein decoupled representations for body and clothing are established based on a uniform shape prior. Building upon this decoupling strategy, we introduce a 3D semantic-confidence strategy aimed at eliminating non-clothing semantic components from the generated clothing. Finally, we employ a 3D implicit deformer, relying on SMPL-X [31] vertex prediction, to optimize the 3D human body, ensuring geometric alignment with clothing of varied shapes.

Limitations. Given the absence of a uniform parametric clothing template, the assessment of matching loss to the body cannot be conducted through differentiable rendering employing a uniform 3D proxy tailored to the generated clothing. Consequently, we opt for a 3D implicit deformation field based on SMPL-X [31] to optimize the alignment between bodies and clothing. While our method enables the fitting of the body to clothing of various shapes, it may yield unnatural matching outcomes when the shapes of the body and clothing differ significantly. In future endeavors, we will employ more accurate deformation proxies combined with object collision detection to optimize the matching of clothing and body bidirectionally in order to achieve better quality of layered generation.

References

[1] FirstName Alpher. Frobnication. *IEEE TPAMI*, 12(1):234–778, 2002.

[2] FirstName Alpher and FirstName Fotheringham-Smythe. Frobnication revisited. *Journal of Foo*, 13(1):234–778, 2003.

[3] FirstName Alpher and FirstName Gamow. Can a computer frobnicate? In *CVPR*, pages 234–778, 2005.

[4] FirstName Alpher, FirstName Fotheringham-Smythe, and FirstName Gamow. Can a machine frobnicate? *Journal of Foo*, 14(1):234–778, 2004.

[5] Hugo Bertiche, Meysam Madadi, and Sergio Escalera. Cloth3d: clothed 3d humans. In *European Conference on Computer Vision*, pages 344–359. Springer, 2020.

[6] Yukang Cao, Yan-Pei Cao, Kai Han, Ying Shan, and Kwan-Yee K Wong. Dreamavatar: Text-and-shape guided 3d human avatar generation via diffusion models. *arXiv preprint arXiv:2304.00916*, 2023. 2

[7] Harvy Clyde Carver, AL O'TOOLE, and TE RAIFORD. *The annals of mathematical statistics*. Edwards Bros., 1930. 5

[8] Enric Corona, Albert Pumarola, Guillem Alenya, Gerard Pons-Moll, and Francesc Moreno-Noguer. Smplicit: Topology-aware generative model for clothed people. In

Proceedings of the IEEE/CVF conference on computer vision and pattern recognition, pages 11875–11885, 2021.

[9] Yao Feng, Jinlong Yang, Marc Pollefeys, Michael J Black, and Timo Bolkart. Capturing and animation of body and clothing from monocular video. In *SIGGRAPH Asia 2022 Conference Papers*, pages 1–9, 2022.

[10] Georgia Gkioxari, Jitendra Malik, and Justin Johnson. Mesh r-cnn. In *Proceedings of the IEEE/CVF international conference on computer vision*, pages 9785–9795, 2019. 2, 7

[11] Fangzhou Hong, Zhaoxi Chen, Yushi Lan, Liang Pan, and Ziwei Liu. Eva3d: Compositional 3d human generation from 2d image collections. *arXiv preprint arXiv:2210.04888*, 2022. 2

[12] Fangzhou Hong, Mingyuan Zhang, Liang Pan, Zhongang Cai, Lei Yang, and Ziwei Liu. Avatarclip: Zero-shot text-driven generation and animation of 3d avatars. *arXiv preprint arXiv:2205.08535*, 2022. 2, 3, 6, 7

[13] Shoukang Hu, Fangzhou Hong, Tao Hu, Liang Pan, Haiyi Mei, Weiye Xiao, Lei Yang, and Ziwei Liu. Humanliff: Layer-wise 3d human generation with diffusion model. *arXiv preprint arXiv:2308.09712*, 2023. 2, 3, 6, 7, 8

[14] Yukun Huang, Jianan Wang, Ailing Zeng, He Cao, Xianbiao Qi, Yukai Shi, Zheng-Jun Zha, and Lei Zhang. Dreamwaltz: Make a scene with complex 3d animatable avatars. *arXiv preprint arXiv:2305.12529*, 2023. 2

[15] Ajay Jain, Ben Mildenhall, Jonathan T Barron, Pieter Abbeel, and Ben Poole. Zero-shot text-guided object generation with dream fields. In *Proceedings of the IEEE/CVF Conference on Computer Vision and Pattern Recognition*, pages 867–876, 2022. 2

[16] Ruixiang Jiang, Can Wang, Jingbo Zhang, Menglei Chai, Mingming He, Dongdong Chen, and Jing Liao. Avatarcraft: Transforming text into neural human avatars with parameterized shape and pose control. *arXiv preprint arXiv:2303.17606*, 2023.

[17] Yuval Kirstain, Adam Polyak, Uriel Singer, Shahbuland Matiana, Joe Penna, and Omer Levy. Pick-a-pic: An open dataset of user preferences for text-to-image generation. *arXiv preprint arXiv:2305.01569*, 2023. 6

[18] Nikos Kolotouros, Thiemo Alldieck, Andrei Zanfir, Eduard Gabriel Bazavan, Mihai Fieraru, and Cristian Sminchisescu. Dreamhuman: Animatable 3d avatars from text. *arXiv preprint arXiv:2306.09329*, 2023. 2

[19] FirstName LastName. The frobnicatable foo filter, 2014. Face and Gesture submission ID 324. Supplied as supplemental material `fg324.pdf`.

[20] FirstName LastName. Frobnication tutorial, 2014. Supplied as supplemental material `tr.pdf`.

[21] Tingting Liao, Hongwei Yi, Yuliang Xiu, Jiaxaing Tang, Yangyi Huang, Justus Thies, and Michael J Black. Tada! text to animatable digital avatars. *arXiv preprint arXiv:2308.10899*, 2023. 2, 3, 6, 7

[22] Chen-Hsuan Lin, Jun Gao, Luming Tang, Towaki Takikawa, Xiaohui Zeng, Xun Huang, Karsten Kreis, Sanja Fidler, Ming-Yu Liu, and Tsung-Yi Lin. Magic3d: High-resolution text-to-3d content creation. In *Proceedings of the IEEE/CVF Conference on Computer Vision and Pattern Recognition (CVPR)*, pages 300–309, 2023. 2

[23] Matthew Loper, Naureen Mahmood, Javier Romero, Gerard Pons-Moll, and Michael J Black. Smpl: A skinned multi-person linear model. In *Seminal Graphics Papers: Pushing the Boundaries, Volume 2*, pages 851–866. 2023. 2, 4

[24] Gal Metzer, Elad Richardson, Or Patashnik, Raja Giryes, and Daniel Cohen-Or. Latent-nerf for shape-guided generation of 3d shapes and textures. In *Proceedings of the IEEE/CVF Conference on Computer Vision and Pattern Recognition*, pages 12663–12673, 2023. 2, 3, 6, 7

[25] Oscar Michel, Roi Bar-On, Richard Liu, Sagie Benaim, and Rana Hanocka. Text2mesh: Text-driven neural stylization for meshes. In *Proceedings of the IEEE/CVF Conference on Computer Vision and Pattern Recognition*, pages 13492–13502, 2022.

[26] Ben Mildenhall, Pratul P Srinivasan, Matthew Tancik, Jonathan T Barron, Ravi Ramamoorthi, and Ren Ng. Nerf: Representing scenes as neural radiance fields for view synthesis. *Communications of the ACM*, 65(1):99–106, 2021. 3, 6

[27] Nasir Mohammad Khalid, Tianhao Xie, Eugene Belilovsky, and Tiberiu Popa. Clip-mesh: Generating textured meshes from text using pretrained image-text models. In *SIGGRAPH Asia 2022 conference papers*, pages 1–8, 2022. 2

[28] Alex Mohr and Michael Gleicher. Building efficient, accurate character skins from examples. *ACM Transactions on Graphics (TOG)*, 22(3):562–568, 2003. 3

[29] Alex Nichol, Prafulla Dhariwal, Aditya Ramesh, Pranav Shyam, Pamela Mishkin, Bob McGrew, Ilya Sutskever, and Mark Chen. Glide: Towards photorealistic image generation and editing with text-guided diffusion models. *arXiv preprint arXiv:2112.10741*, 2021. 2

[30] Georgios Pavlakos, Vasileios Choutas, Nima Ghorbani, Timo Bolkart, Ahmed AA Osman, Dimitrios Tzionas, and Michael J Black. Expressive body capture: 3d hands, face, and body from a single image. In *Proceedings of the IEEE/CVF conference on computer vision and pattern recognition*, pages 10975–10985, 2019. 3

[31] Georgios Pavlakos, Vasileios Choutas, Nima Ghorbani, Timo Bolkart, Ahmed AA Osman, Dimitrios Tzionas, and Michael J Black. Expressive body capture: 3d hands, face, and body from a single image. In *Proceedings of the IEEE/CVF conference on computer vision and pattern recognition*, pages 10975–10985, 2019. 2, 5, 9

[32] Yicong Peng, Yichao Yan, Shengqi Liu, Yuhao Cheng, Shanyan Guan, Bowen Pan, Guangtao Zhai, and Xiaokang Yang. Cagenerf: Cage-based neural radiance field for generalized 3d deformation and animation. *Advances in Neural Information Processing Systems*, 35:31402–31415, 2022.

[33] Ben Poole, Ajay Jain, Jonathan T Barron, and Ben Mildenhall. Dreamfusion: Text-to-3d using 2d diffusion. *arXiv preprint arXiv:2209.14988*, 2022. 2

[34] Ben Poole, Ajay Jain, Jonathan T Barron, and Ben Mildenhall. Dreamfusion: Text-to-3d using 2d diffusion. *arXiv preprint arXiv:2209.14988*, 2022. 2

[35] Alec Radford, Jong Wook Kim, Chris Hallacy, Aditya Ramesh, Gabriel Goh, Sandhini Agarwal, Girish Sastry, Amanda Askell, Pamela Mishkin, Jack Clark, et al. Learning

transferable visual models from natural language supervision. In *International conference on machine learning*, pages 8748–8763. PMLR, 2021. 2

[36] Alec Radford, Jong Wook Kim, Chris Hallacy, Aditya Ramesh, Gabriel Goh, Sandhini Agarwal, Girish Sastry, Amanda Askell, Pamela Mishkin, Jack Clark, et al. Learning transferable visual models from natural language supervision. In *International conference on machine learning*, pages 8748–8763. PMLR, 2021.

[37] Amit Raj, Srinivas Kaza, Ben Poole, Michael Niemeyer, Nataniel Ruiz, Ben Mildenhall, Shiran Zada, Kfir Aberman, Michael Rubinstein, Jonathan Barron, et al. Dreambooth3d: Subject-driven text-to-3d generation. *arXiv preprint arXiv:2303.13508*, 2023. 2

[38] Elad Richardson, Gal Metzer, Yuval Alaluf, Raja Giryes, and Daniel Cohen-Or. Texture: Text-guided texturing of 3d shapes. *arXiv preprint arXiv:2302.01721*, 2023.

[39] Robin Rombach, Andreas Blattmann, Dominik Lorenz, Patrick Esser, and Björn Ommer. High-resolution image synthesis with latent diffusion models. In *Proceedings of the IEEE/CVF conference on computer vision and pattern recognition*, pages 10684–10695, 2022. 2, 3, 6

[40] Chitwan Saharia, William Chan, Saurabh Saxena, Lala Li, Jay Whang, Emily Denton, Seyed Kamyar Seyed Ghasemipour, Burcu Karagol Ayan, S Sara Mahdavi, Rapha Gontijo Lopes, et al. Photorealistic text-to-image diffusion models with deep language understanding, 2022. *URL https://arxiv. org/abs/2205.11487*, 4. 2

[41] Chitwan Saharia, William Chan, Saurabh Saxena, Lala Li, Jay Whang, Emily L Denton, Kamyar Ghasemipour, Raphael Gontijo Lopes, Burcu Karagol Ayan, Tim Salimans, et al. Photorealistic text-to-image diffusion models with deep language understanding. *Advances in Neural Information Processing Systems*, 35:36479–36494, 2022. 3

[42] Aditya Sanghi, Hang Chu, Joseph G Lambourne, Ye Wang, Chin-Yi Cheng, Marco Fumero, and Kamal Rahimi Malekshan. Clip-forge: Towards zero-shot text-to-shape generation. In *Proceedings of the IEEE/CVF Conference on Computer Vision and Pattern Recognition*, pages 18603–18613, 2022. 2

[43] Gusi Te, Xiu Li, Xiao Li, Jinglu Wang, Wei Hu, and Yan Lu. Neural capture of animatable 3d human from monocular video. In *European Conference on Computer Vision*, pages 275–291. Springer, 2022. 2

[44] Nanyang Wang, Yinda Zhang, Zhuwen Li, Yanwei Fu, Wei Liu, and Yu-Gang Jiang. Pixel2mesh: Generating 3d mesh models from single rgb images. In *Proceedings of the European conference on computer vision (ECCV)*, pages 52–67, 2018. 2

[45] Peng Wang, Lingjie Liu, Yuan Liu, Christian Theobalt, Taku Komura, and Wenping Wang. Neus: Learning neural implicit surfaces by volume rendering for multi-view reconstruction. *arXiv preprint arXiv:2106.10689*, 2021. 6

[46] Zhenzhen Weng, Zeyu Wang, and Serena Yeung. Zeroavatar: Zero-shot 3d avatar generation from a single image. *arXiv preprint arXiv:2305.16411*, 2023. 2

[47] Yuliang Xiu, Jinlong Yang, Xu Cao, Dimitrios Tzionas, and Michael J Black. Econ: Explicit clothed humans obtained from normals. *arXiv preprint arXiv:2212.07422*, 2022. 2

[48] Jiale Xu, Xintao Wang, Weihao Cheng, Yan-Pei Cao, Ying Shan, Xiaohu Qie, and Shenghua Gao. Dream3d: Zero-shot text-to-3d synthesis using 3d shape prior and text-to-image diffusion models. In *Proceedings of the IEEE/CVF Conference on Computer Vision and Pattern Recognition (CVPR)*, pages 20908–20918, 2023.

[49] Tianhan Xu and Tatsuya Harada. Deforming radiance fields with cages. In *European Conference on Computer Vision*, pages 159–175. Springer, 2022.

[50] Zhitao Yang, Zhongang Cai, Haiyi Mei, Shuai Liu, Zhaoxi Chen, Weiye Xiao, Yukun Wei, Zhongfei Qing, Chen Wei, Bo Dai, et al. Synbody: Synthetic dataset with layered human models for 3d human perception and modeling. *arXiv preprint arXiv:2303.17368*, 2023.

[51] Kim Youwang, Kim Ji-Yeon, and Tae-Hyun Oh. Clip-actor: Text-driven recommendation and stylization for animating human meshes. In *European Conference on Computer Vision*, pages 173–191. Springer, 2022.

[52] Yu-Jie Yuan, Yang-Tian Sun, Yu-Kun Lai, Yuewen Ma, Rongfei Jia, and Lin Gao. Nerf-editing: geometry editing of neural radiance fields. In *Proceedings of the IEEE/CVF Conference on Computer Vision and Pattern Recognition*, pages 18353–18364, 2022.

[53] Jianfeng Zhang, Zihang Jiang, Dingdong Yang, Hongyi Xu, Yichun Shi, Guoxian Song, Zhongcong Xu, Xinchao Wang, and Jiashi Feng. Avatargen: a 3d generative model for animatable human avatars. In *European Conference on Computer Vision*, pages 668–685. Springer, 2022. 2

[54] Zerong Zheng, Tao Yu, Yebin Liu, and Qionghai Dai. Pamir: Parametric model-conditioned implicit representation for image-based human reconstruction. *IEEE transactions on pattern analysis and machine intelligence*, 44(6): 3170–3184, 2021. 6